Sheffield Hallam University

Use of laser interferometry for measuring concrete substrate roughness in patch repairs

GRIGORIADIS, Konstantinos

Available from Sheffield Hallam University Research Archive (SHURA) at:

http://shura.shu.ac.uk/11474/

This document is the author deposited version. You are advised to consult the publisher's version if you wish to cite from it.

Published version

GRIGORIADIS, Konstantinos (2016). Use of laser interferometry for measuring concrete substrate roughness in patch repairs. Automation in Construction, 64, 27-35.

Sheffield Hallam University Research Archive
http://shura.shu.ac.uk

Use of laser interferometry for measuring concrete substrate roughness in patch repairs

Konstantinos Grigoriadis[1,2*]

[1]School of Engineering and Mathematical Sciences, City University, Northampton Square, London, EC1V 0HB, UK

[2]Centre for Infrastructure Management, Materials & Engineering Research Institute, Sheffield Hallam University, Howard Street, Sheffield, S1 1WB, UK (*Corresponding Author. Tel: +44 114 225 5075; Email: k.grigoriadis@shu.ac.uk)

Abstract

The overall success and long-term durability of a patch repair is significantly influenced by the bond developed at the interface between the concrete substrate and the repair material. In turn, the bond strength is influenced by the topography (roughness) of the substrate surface after removal of the defective concrete. However, different removal methods of defective concrete produce substrate surfaces with different topographies. Hence, the ability to measure and characterise the topography of substrate surfaces is of great importance for evaluating the effectiveness of different removal methods. In this paper, the effect of two removal methods: electric chipping hammers and Remote Robotic Hydro-erosion (RRH) on the surface roughness is investigated through the use of a prototype non-contact (optical) laser interferometry measuring device. Laboratory results show that the above equipment can be used to characterise substrate roughness and confirm the ability of RRH to create rougher surfaces as opposed to chipping hammers.

Keywords

Concrete, Remote robotic hydro-erosion, Substrate surface roughness, Patch repair

Nomenclature

CV	Coefficient of variation (%)
d	Mean diameter of the circular area in sand patch method (mm)
D_a	Average double amplitude of an irregular wave (mm)
$\dfrac{dz}{dx}$	Local slope of the surface profile
L	Evaluation length along the *x* axis (mm)
Lo	Actual profile length (mm)
Lr	Profile length ratio (-)
RG	Roughness gradient (mm)
RI	Roughness index of sand patch method (mm)
*RΔ*a	Average absolute slope (rad)
RΔq	Root mean square average slope (rad)
SD	Standard deviation
Δ	Distance between measuring consecutive points (mm)
$\bar{x}$	Population mean
2α	Double amplitude of a saw-toothed curve (mm)

1. Introduction

  Surface roughness has a different meaning in different fields of Science and Engineering. In the field of concrete patch repairs, surface roughness can be used to describe the topography of the concrete substrate prior to the application of repair. The overall success and long-term durability of a concrete patch repair is highly dependent upon the interface bond between the concrete substrate and the repair material. Interface bond consists of mechanical interlocking and adhesion. The effect of mechanical interlocking is determined by the surface roughness of the substrate, whereas, adhesion is created by the development of chemical bonds between

the hardened concrete substrate and the paste of the repair material. Hence, adhesion is influenced by the factors that generally influence aggregate-paste bond as highlighted by Neville [1] and Mindess et al. [2]. Although, adhesion develops as the repair material cures, the contribution of mechanical interlocking stays the same with age. However, increased surface roughness results in improved mechanical interlocking which in turn increases the interface bond. Hence, more surface area is available for the paste to adhere and together with mechanical interlocking it increases the bond strength [3].

The surface roughness needs to be measured and characterised in order to study its influence on the bond between concrete substrate and the repair material. However, with the exception of sand patch and contact (stylus) profilometry methods [4-7], no other method has been standardised by BS EN 1504-10 [4] for use in the field of concrete patch repairs.

The sand patch method is based on measuring the mean peak-to-valley height known as Roughness Index (*RI*) of a horizontal surface. For this purpose, 25 ml of dry sand is distributed in a circular configuration on the surface to be measured in such a way that all cavities are just filled. Next, the mean of 3 measured diameters in mm taken at three equally spaced positions around the circumference of the circular area covered by the sand is obtained as shown in Fig. 1. Finally, the Roughness Index is calculated by eq. (1) [4].

$$RI = \frac{31800}{d^2} \tag{1}$$

where *RI* is the roughness index (mm) and *d* is the mean diameter of the circular area (mm).

The sand patch method is quick, inexpensive and very simple to perform on site. However, it is very crude and sensitive to operator error.
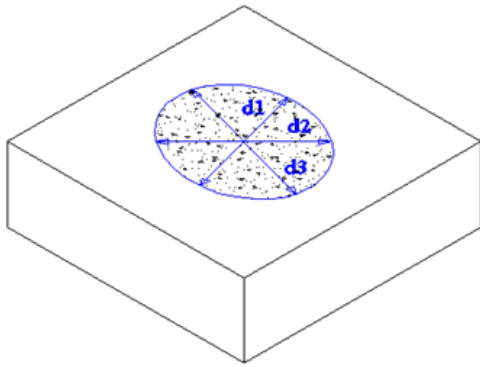
Fig. 1. Schematic diagram of sand patch method.

Contact profilometry method on the other hand, is based on the use of diamond stylus instruments which move along a predetermined horizontal path and record vertical deflection as a function of position as shown in Fig. 2. Typical stylus profilometers can measure small vertical deflections (10 nm to 1 mm) in relatively small industrial components such as screw threads, gear shafts, and valves making them unsuitable for measuring concrete substrate roughness. In addition, like the sand patch method, it requires contact with the substrate to be characterised and its application is limited to horizontal surfaces.
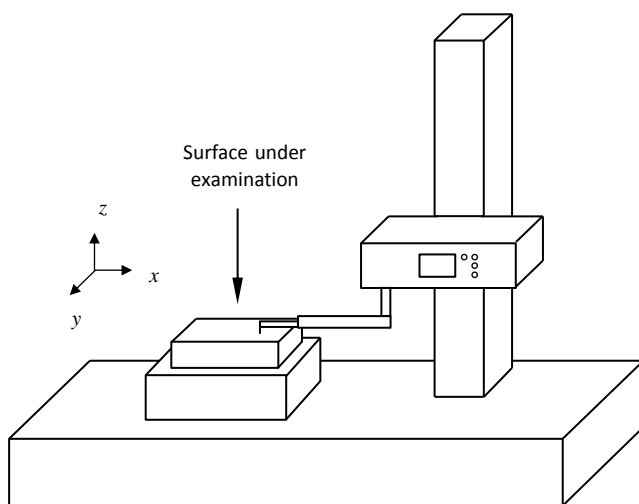

Fig. 2. Schematic diagram of a typical contact (stylus) profilometer.

A number of methods are available for measuring and characterising the surface roughness of concrete pavements. Holt and Musgrove [8] provide a detailed review of these methods.

The surface roughness of concrete substrates can be characterised by comparing them with standard Concrete Surface Profiles (CSP) which have been produced by ICRI in the form of nine plastic model surfaces [9]. These profiles replicate different levels of surface roughness obtained by different methods of concrete removal. Each profile is assigned a CSP number starting from CSP1 (acid etched/almost flat) up to CSP9 (heavily scarified/very rough).

ASTM D7682 [10] describes a method to obtain a permanent record of a concrete surface that has been abraded or roughened. For this purpose, a replica putty is used to obtain a replica coupon of the concrete surface. Next, the replica coupon is either visually compared to the nine plastic model surfaces produced by ICRI [9] or it is measured by a specially designed micrometre to determine its depth.

Silfwerbrand [11] proposed a different method for measuring and characterising surface roughness by developing an automatic laser profilometry equipment. His method was based on approximating the measured surface profile by a saw-toothed curve as shown in Fig. 3. Double amplitude 2α was used as the main surface roughness parameter and was evaluated for different values of the distance Δ between consecutive measuring points using eq. (2).

$$2a = \frac{1}{n-1}\sum_{j=1}^{n-1}|z_{j+1} - z_j| \tag{2}$$

where 2α is the double amplitude of the saw-toothed curve (mm); Δ is the distance between consecutive measuring points; $z_1, z_2, z_{3...}z_j$ are the z co-ordinates of points 1, 2, 3…j.
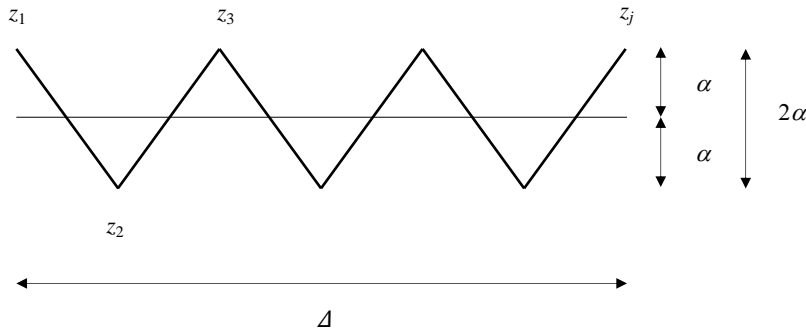
Fig. 3. Schematic diagram of saw-toothed roughness profile used by Silfwerbrand [11] for evaluating surface roughness.

Abu-Tair et al. [12] used a two-dimensional profile texture metre to measure and characterise surface roughness. The profile texture metre consisted of 500 needles spaced 1 mm apart, each 0.8 mm in diameter. The needles were allowed to fall on the surface under investigation and hence replicate its profile. A photograph was then taken of the profile. By enlarging the photograph, measurements were obtained which defined the texture depth of the concrete surface. The profile of the surface was treated as a series of irregular waves with each wave having its own wavelength and minimum and maximum amplitude. Next, the average double amplitude (D_a) for each wave was evaluated. Finally, by averaging the values of D_a for all irregular waves, a roughness parameter known as roughness gradient (RG) was determined.

Maerz et al. [13] developed an experimental hand-held laser profilometry scanner to measure the surface roughness of concrete substrates prior to FRP laminate application. It was based on the principles of Schmaltz light-section microscope and the method of shadow profilometry also known as laser striping. The captured image was transformed into a series of eleven profiles in the *x-y* plane. Each profile was then measured by using $R\Delta a$ roughness parameter described in Section 2.5.

Ahmed and Haas [14] used closed range digital photogrammetry to accurately reconstruct a detailed 3D model of a pavement surface. For this purpose, a non-metric DSLR CMOS

camera with built-in flash was used. Their results demonstrated the potential of using photogrammetry for crack detection and 3D surface reconstruction. Photogrammetry is simple to perform, has a relatively low cost and the accuracy of the 3D surface model can be improved by adding new photographs taken from different positions [15]. However, it should be noted that the accuracy of the 3D model is significantly affected by the type of camera used and its specifications, number of photos used and position where these were taken [15].

Finally, over the last 5 years, a number of researchers [16-20] used both experimental and commercial 3D laser scanners based on triangulation method to assess the surface of either asphalt pavements or concrete substrates. They are based on a laser emitter which produces a beam of energy that hits a point on the surface of the object under investigation. Next, the reflected light is measured with the aid of a CCD or CMOS sensor. By repeating the procedure for all points on the surface of the object it is possible to obtain their co-ordinates using basic trigonometric equations and construct a 3D point cloud of the surface [17]. Once a 3D model of the surface is obtained, it can be analysed using a number of 3D roughness parameters.

2. Experimental programme

2.1. Details of mixes and slab specimens

A laboratory research based on the use of prototype non-contact equipment (described in Section 2.6) was carried out in order to measure and characterise the surface roughness of concrete surfaces prior to patch repairs and at the same time check the ability of Remote Robotic Hydro-erosion (RRH) to produce much rougher surfaces compared to chipping hammers. Sixty concrete slab specimens with dimensions of 400 x 400 x 125 mm were produced in six groups. The first four groups consisted of six mixes each. Group five consisted of three mixes, whereas group six consisted of five mixes. Thirty-two concrete

mixes were produced in total. One, two or three slabs together with the required number of 100 mm cubes for determining 28 day strength were produced from each mix. The w/c ratios of groups 1, 2, 3, 4, 5 and 6 were 0.4, 0.45, 0.50, 0.55, 0.4 and 0.45, respectively. At 28 days age, concrete was removed from the trowelled surface of the slabs using an electric chipping hammer or RRH as described in Section 2.4. Details of all slab mixes are shown in Table 1.

Table 1
Details of slabs.

Slab group	Mix number	Slab number	w/c ratio	Strength* (MPa)	Concrete removal method
1	1-6	S1-S12	0.40	54.0-58.0	Chipping hammer
2	7-12	S13-S24	0.45	47.5-53.5	Chipping hammer
3	13-18	S25-S36	0.50	41.0-46.0	Chipping hammer
4	19-24	S37-S48	0.55	37.0-41.0	Chipping hammer
5	25-27	PL2, PL14, P1	0.40	54.0-64.0	RRH
6	28-32	PL5, PL6, PL9, PL10, PL11 PL13, PL15, PL16, P5	0.45	48.0-53.0	RRH

* 28 day compressive strength.

2.2. Materials

The specimens were produced using OPC CEM I 42.5 N conforming to BS EN 197-1: 2000 [21], coarse sharp sand (50% passing a 600 μm sieve), and uncrushed river gravel with maximum coarse size of 10 mm. The mix design was based on the guidelines of BRE [22].

2.3. Casting and curing of slab specimens

The specimens were cast in timber moulds and compacted on a vibrating table. After the concrete had set, the moulds were covered with damp rags. The specimens were de-moulded 24 hours after casting and placed in water. After 6 days in water, the specimens were air-cured in a storage room for 21 days at 19 $^{\circ}$C, 50-60% RH.

2.4. Surface preparation

A layer of approximately 25-30 mm was removed from the top (trowelled) surface of slabs S1-S48 using a Kango Type 950 electric hammer which simulated the action of pneumatic chipping hammers commonly used in the construction industry. In the remaining twelve slab specimens (PL2, PL5, PL6, PL9-PL11, PL13-PL16, P1 and P5) a layer of approximately 25-30 mm was removed using Remote Robotic Hydro-erosion (RRH). RRH is a precise form of robotic hydro-demolition that takes advantage of remote robotic technology and uses sensor feedback to control better the quality and quantity of concrete removal [23-24]. A panoramic view of all specimens is shown in Fig. 4.
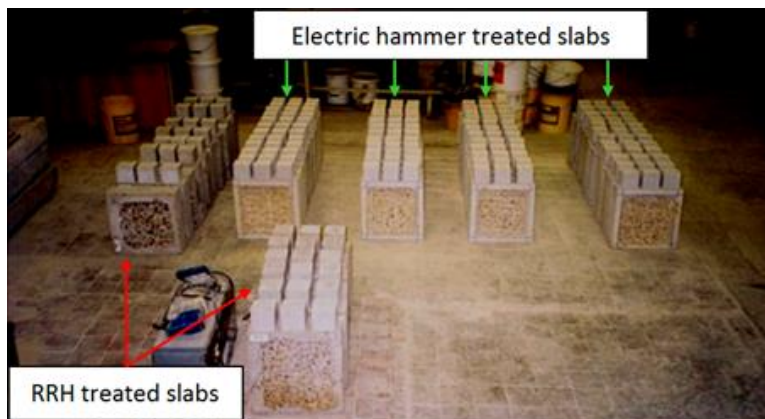
Fig. 4. Concrete substrate surfaces obtained using either RRH or an electric hammer.

2.5. Selection of roughness parameters

The first step in measuring and characterising concrete substrate surfaces is the acquisition of a satisfactory profile. Once an adequate profile is obtained, it should be analysed and characterised using some form of roughness index or parameter. Unfortunately, there is no universal number, descriptor or parameter that can be used to analyse and characterise the topography of a surface. A large number of two-dimensional (2D) and three-dimensional (3D) roughness parameters have been developed to characterise the roughness of a surface for applications in various fields of Science and Engineering. Gadelmawla et al. [25] provide

a review of the 2D parameters, whereas Griffiths [26] and Bewoor and Kulkarni [27] provide a detailed review of both 2D and 3D parameters.

In the field of concrete patch repairs, the bond strength is considerably influenced by the topography (roughness) of the substrate surface obtained after removal of the defective concrete. Hence, roughness parameters which influence the surface contact area available between concrete substrates and repair materials should be chosen and evaluated. Based on the above criterion, 2D roughness parameters which are important for mechanical interlocking [13, 25-27] are evaluated for the surface profile shown in Fig. 5.

The average slope $R\Delta a$ is evaluated by first calculating the slope between two successive points of the surface profile as shown in Fig. 5. Next, the average of these slopes is evaluated. $R\Delta q$ is the root mean square of the average slope. Both $R\Delta a$ and $R\Delta q$ parameters are important to determine the mechanical interlocking property. A surface with higher $R\Delta a$ and $R\Delta q$ values provides better mechanical interlocking than a surface with lower values. Lr is the ratio of the actual profile length Lo and the evaluation length L. A surface with high peaks and deep valleys has a higher Lo and hence a higher Lr value compared to a surface with low peaks and shallow valleys. Thus more surface area is available for the repair material to adhere at higher Lr values.
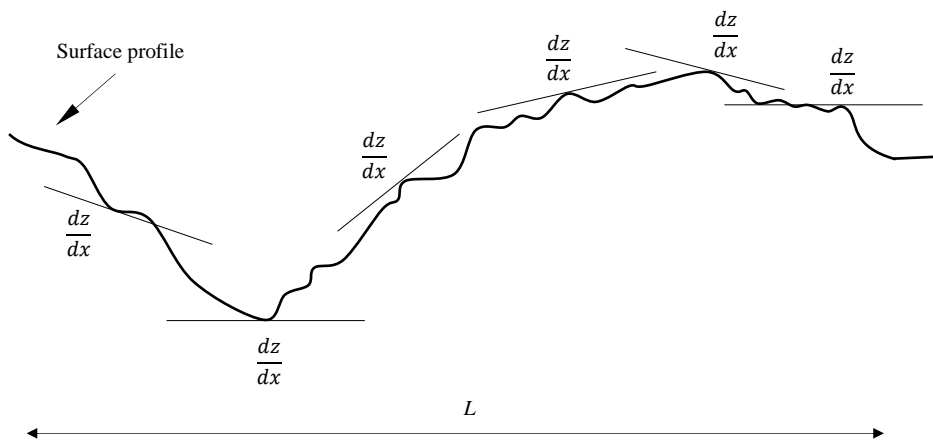

Fig. 5. Local slopes along the surface profile.

The following equations can be used to determine these roughness parameters [26-27]:

Parameter 1: Average absolute slope $R\varDelta a$

$$R\varDelta a = \frac{1}{L}\int_0^L \left|\frac{dz}{dx}\right| dx \tag{3}$$

or in discretised form

$$R\varDelta a = \frac{1}{L}\sum_{n=1}^N |z_{n+1} - z_n| \tag{4}$$

Parameter 2: Root mean square average slope $R\varDelta q$

$$R\varDelta q = \sqrt{\frac{1}{L}\int_0^L \left(\frac{dz}{dx}\right)^2 dx} \tag{5}$$

or in discretised form

$$R\varDelta q = \sqrt{\frac{1}{L}\sum_{n=1}^N (z_{n+1} - z_n)^2} \tag{6}$$

Parameter 3: Profile length ratio Lr

$$Lr = \frac{Lo}{L} = \frac{1}{L}\int_0^L \sqrt{1 + \left(\frac{dz}{dx}\right)^2} dx \tag{7}$$

or in discretised form

$$Lr = \frac{Lo}{L} = \frac{1}{L}\sum_{n=1}^N \sqrt{\left(\frac{L}{N}\right)^2 + (z_{n+1} - z_n)^2} \tag{8}$$

where $R\varDelta a$ is the average absolute slope (rad), $R\varDelta q$ is the root mean square average slope (rad), Lr is the profile length ratio, $\frac{dz}{dx}$ is the local slope of the surface profile, Lo is the actual profile length (mm), and L is the evaluation length along the x axis (mm).

2.6. Surface roughness measuring equipment

An experimental 3D interferometric fringe-based imaging system for surface profiling, positioning and control for space applications developed by Meggitt et al. [28] was used to

characterise the substrate surfaces. The method belongs to a group of non-contact (optical) techniques known as phase measurement interferometry.

The measuring system consists of a fringe projector, a C-Cam Technologies Model CCi4 digital camera (sensor type: IBIS4 CMOS, total light-sensitive pixels: 1310720 (1280 Horizontal x 1024 Vertical), pixel pitch: 7 x 7 μm, frame speed full resolution: approximately 7.5 frames/s, operating temperature: 0 to +50 ^{o}C), a control system for the laser diode and a computer for processing the data. The fringe projector illuminates the surface of the object under investigation with a set of vertical interference fringes through an illumination cone as shown in Fig. 6 (a-c). Projected fringes having cosine intensity profiles are used. Next, the pattern of the projected fringes on the surface of the object is analysed to determine the co-ordinates of points on the surface. The aim of using projected fringes, instead of a scanning spot or line, is that data for all points in an image plane can be captured simultaneously, hence reducing the image acquisition time. The fringe projector, object and camera remain stationary during measurement [28].

The distance between the laser projector and the surface of the object is limited to a minimum of 0.5 m and a maximum of 5 m due to the sensitivity of the camera and the power of the projector. The camera distance from the surface of the object is similar to that of the projector. In the case of the concrete substrate slabs, the camera and the projector were positioned at a distance of approximately 2 m from their surface. The time required to measure a single specimen involved the acquisition of only 6 image frames and was done in approximately 2 s.

Two software modules (data acquisition module and data processing module) are used for control and data processing purposes. Data acquisition module is responsible for controlling the camera, image averaging and phase stepping of the fringe projector. Data processing module is responsible for analysing images and performing all necessary calculations to

12

produce the x, y and z co-ordinates of the surface points [28]. The equipment can capture and analyse a square area of approximately 140 x 140 mm on the x-y plane. Both x and y axes are divided into 251 points, resulting in a spacing length of approximately 0.5 mm, in a very fine square mesh consisting of 251 lines on both x and y axes and a total of 63001 points. Next, the z-coordinates of the 63001 points are generated and stored in a matrix form. Once the image is captured and analysed, a very detailed and accurate 3D topography of the surface is created using Mathcad software as shown in Fig. 7. This is one of the big advantages of the above system compared with the Sand Patch method and Contact Stylus profilometers. Finally, the z axis coordinates of the 63001 points can be processed using computer software such as Mathcad or Matlab to calculate various 2D roughness parameters on either x or y axis. The 2D parameters $R\Delta a$, $R\Delta q$ and Lr, described in Section 2.5 were used to calculate the surface roughness of the substrate samples. Computer programmes for evaluating each one of them, along the x axis of the specimens, were written in Matlab.

(a)

(b)

(c)
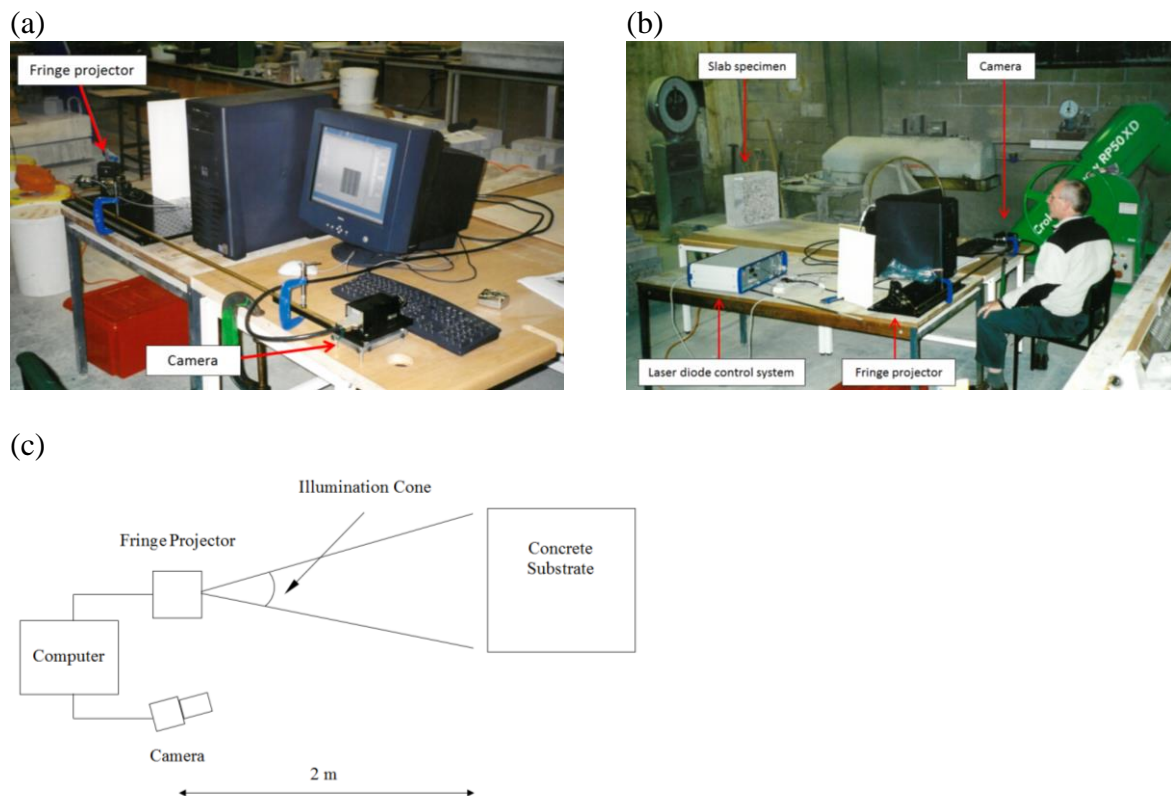
Fig. 6 (a-c). Schematic diagram of fringe-based laser interferometry equipment used to measure surface roughness of the concrete substrates.
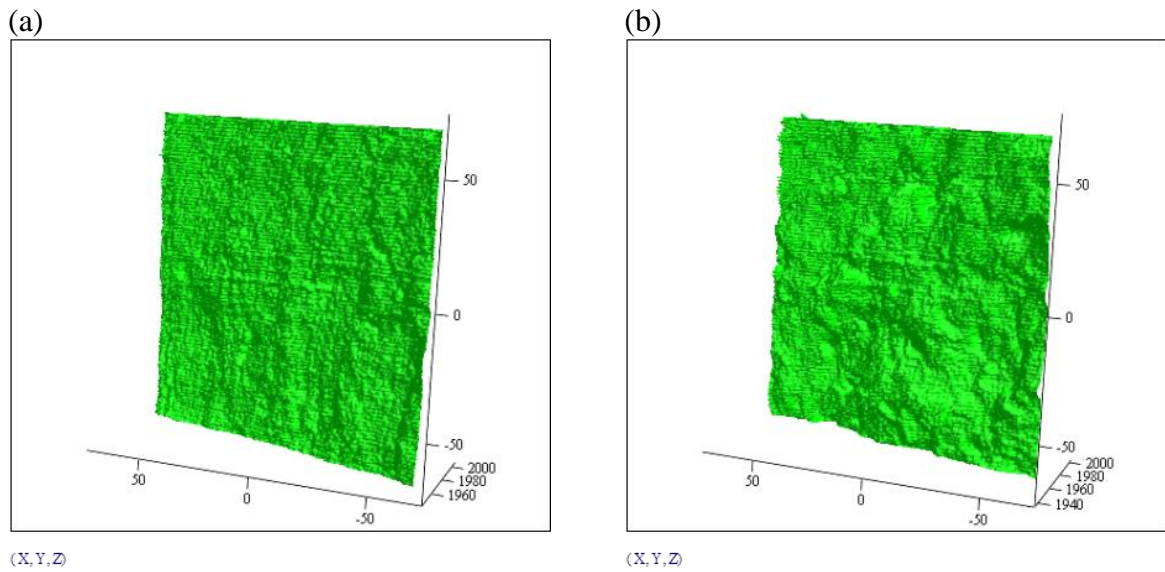
13

Fig. 7. Typical 3D surfaces obtained using (a) an electric hammer and (b) Remote Robotic Hydro-erosion.

3. Results and discussion

Initially, 3D images of the excavated surface of the 60 slab specimens were created using the fringe-based laser interferometry equipment. Next, $R\Delta$a, $R\Delta q$ and Lr roughness parameters were calculated for every mesh line parallel to the x axis and an average roughness value based on the results of 251 such lines was obtained for each slab. In addition, 2α roughness parameter proposed by Silfwerbrand [11] was evaluated. The measured values of all concrete substrate surfaces (produced using either an electric hammer or RRH) are shown in Figs. 8-11. A summary of all the above results is provided in Table 2. As shown in Table 2, all four 2D roughness parameters were able to distinguish between surfaces obtained by the two removal methods and confirm that RRH produces rougher surfaces which can promote bond strength. When $R\Delta$a parameter was employed, RRH showed an average increase in surface roughness of 21% along the x axis. RRH showed an average increase of 24% along the x axis when $R\Delta q$ parameter was used. When Lr was considered, RRH yielded

14

an average increase in surface roughness of 10% along the x axis. Finally, when 2α was used,
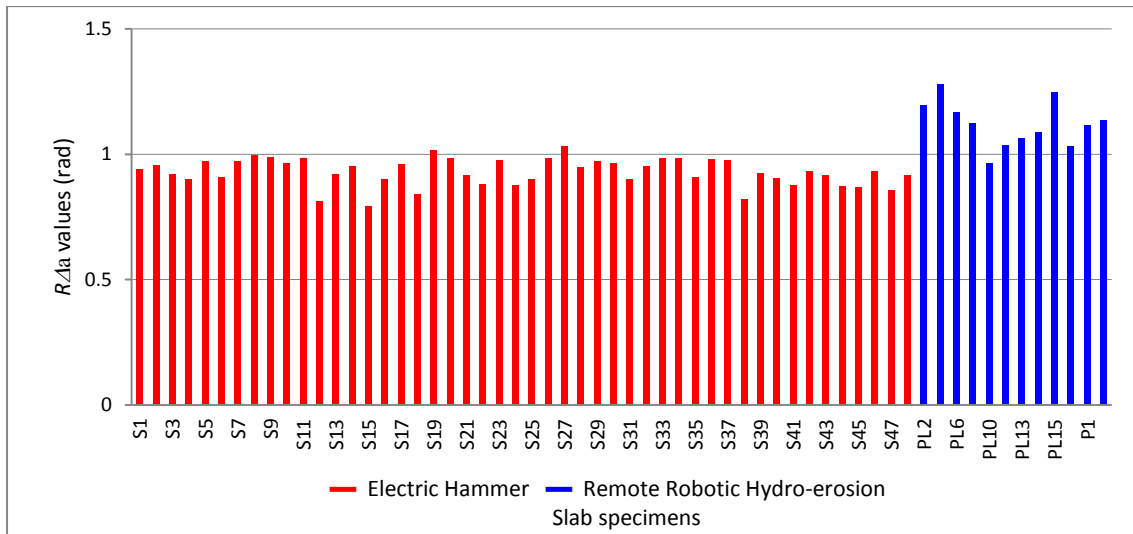
RRH showed an average increase in surface roughness of 19%.

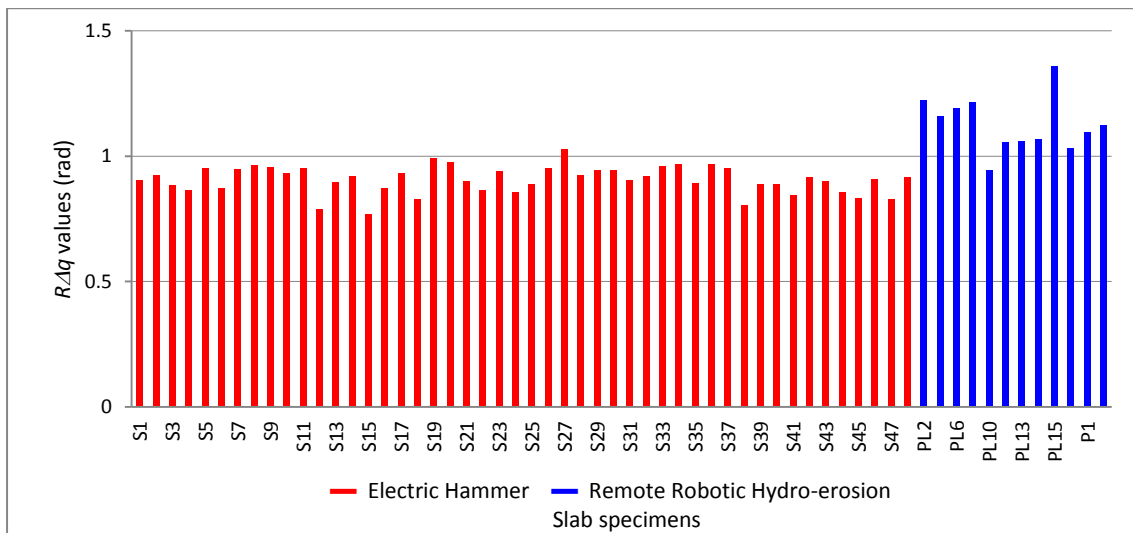**Fig. 8.** $R\varDelta a$ values (rad) measured along the x axis.

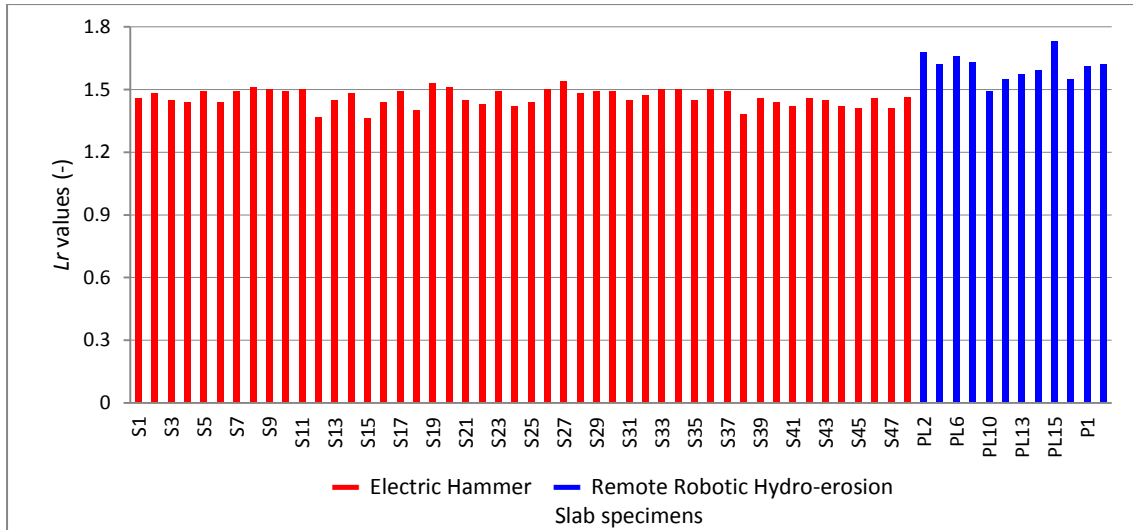**Fig. 9.** $R\varDelta q$ values (rad) measured along the x axis.

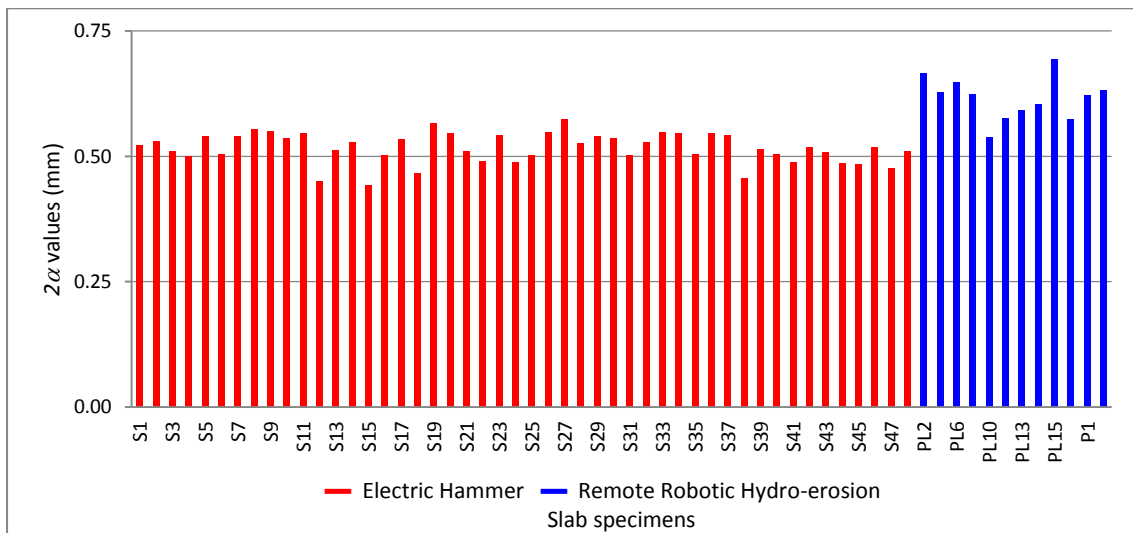**Fig. 10.** *Lr* values (-) measured along the *x* axis.

Fig. 11. *2α* values (mm) measured along the *x* axis.

Table 2
Values of *RΔ*a, *RΔq*, *Lr* and *2α* roughness parameters of electric hammer and RRH prepared surfaces.

Roughness parameter	Range of values		Mean values		% increase with RRH
	Electric hammer surfaces	RRH surfaces	Electric hammer surfaces	RRH surfaces	
*RΔ*a (rad)	0.79-1.03	0.97-1.28	0.93	1.12	21
RΔq (rad)	0.77-1.03	0.95-1.36	0.91	1.13	24
Lr (-)	1.36-1.54	1.49-1.73	1.46	1.61	10
2α (mm)	0.44-0.57	0.54-0.69	0.52	0.62	19

In addition, the effect of substrate compressive strength (w/c ratios of 0.4 and 0.45) on the percentage increase with RRH was investigated for electric hammer and RRH treated slabs cast at the same grade. Very similar results were observed for both w/c ratios as shown in Table 3, indicating no significant effect of w/c ratio on roughness within the range of 0.4-0.45.

Table 3
Effect of substrate strength on percentage increase with RRH.

Roughness parameter	w/c ratio	Range of values		Mean values		% increase with RRH
		Electric hammer surfaces	RRH surfaces	Electric hammer surfaces	RRH surfaces	
$R\Delta a$ (rad)	0.40	0.81-1.00	1.09-1.20	0.94	1.13	20
	0.45	0.79-1.02	0.97-1.28	0.92	1.12	22
$R\Delta q$ (rad)	0.40	0.79-0.96	1.07-1.22	0.91	1.13	24
	0.45	0.77-0.99	0.95-1.36	0.90	1.13	26
Lr (-)	0.40	1.37-1.51	1.59-1.68	1.47	1.63	11
	0.45	1.36-1.53	1.49-1.73	1.45	1.60	10
$2a$ (mm)	0.40	0.45-0.55	0.60-0.67	0.52	0.63	21
	0.45	0.44-0.57	0.54-0.69	0.51	0.61	20

Finally, it should be noted that the level of surface roughness obtained using electric chipping hammers may be affected by the sharpness and length of the chipping attachment as well as the level of vibration frequency at which it operates. Hence, by carefully investigating the above parameters an improvement on roughness values obtained using electric chipping hammers may be possible.

$R\Delta a$, $R\Delta q$, Lr and 2α values for both types of surfaces were also plotted in the form of histograms to observe their distribution. These are shown in Fig. 12 (a-h) together with the values for the mean ($\bar{x}$) standard deviation (SD) and coefficient of variation (CV). As expected, all roughness parameters for both surfaces correspond in general to standard normal distributions.
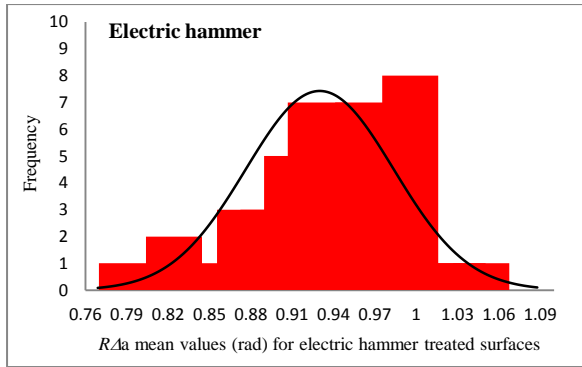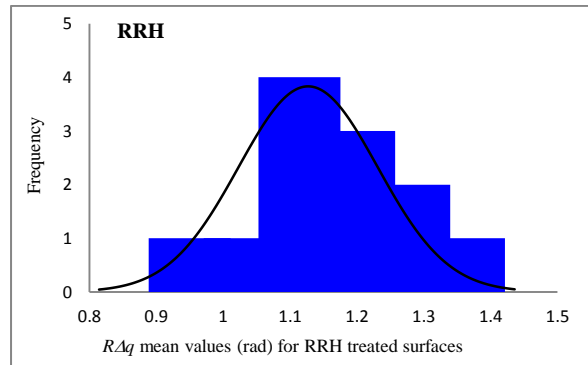
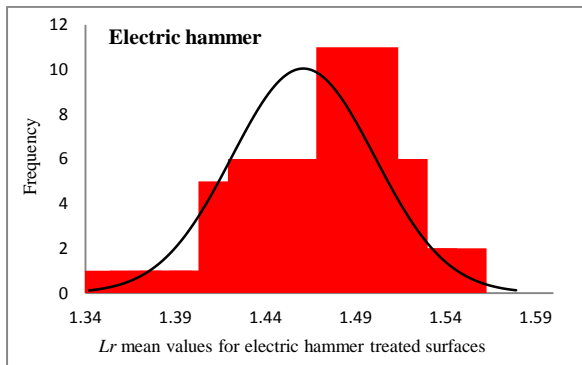a) $\bar{x} = 0.93$ rad, $SD = 0.054$ rad, $CV = 5.81\%$
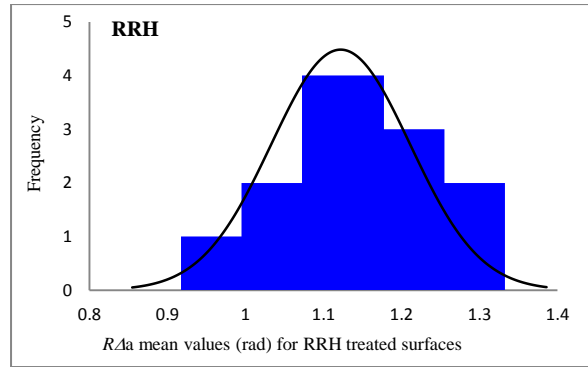
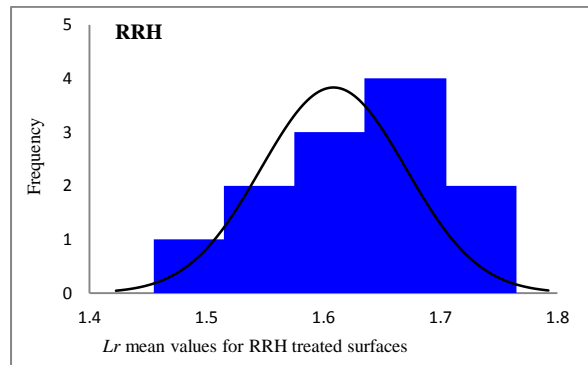b) $\bar{x} = 1.12$ rad, $SD = 0.092$ rad, $CV = 8.24\%$
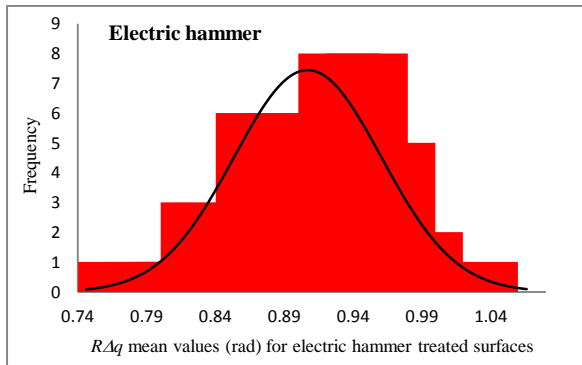
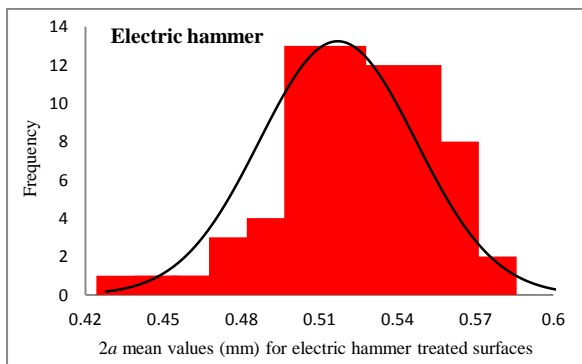c) $\bar{x} = 0.91$ rad, $SD = 0.054$ rad, $CV = 5.97\%$

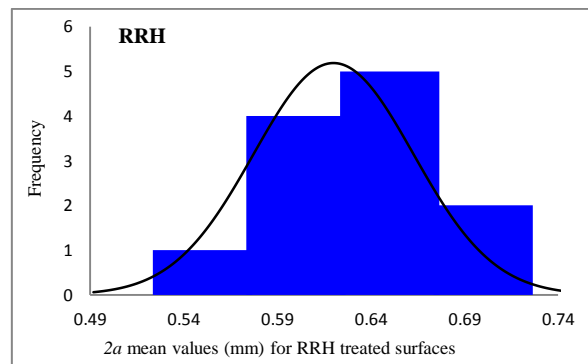d) $\bar{x} = 1.13$ rad, $SD = 0.109$ rad, $CV = 9.71\%$

e) $\bar{x} = 1.46$, $SD = 0.040$, $CV = 2.75\%$

f) $\bar{x} = 1.61$, $SD = 0.065$, $CV = 4.02\%$

g) $\bar{x} = 0.52$ mm, $SD = 0.030$ mm, $CV = 5.76\ \%$

h) $\bar{x} = 0.62$ mm, $SD = 0.043$ mm, $CV = 6.93\ \%$

Fig. 12 (a-h). Histogram plots of $R\Delta a$, $R\Delta q$, Lr and 2α for electric hammer and RRH prepared surfaces.

4. Conclusions

The following conclusions can be drawn from the present laboratory-based investigation on measuring concrete substrate surface roughness prior to patch repair.

- A non-contact fringe-based laser interferometry imaging technique suitable for potential on-site application can be used to create a very accurate 3D digital profile of a concrete substrate surface regardless of its orientation (horizontal, vertical or overhead).

- 2D roughness parameters $R\Delta a$, $R\Delta q$, Lr and 2α can be employed to measure the substrate surface roughness. They confirm the ability of Remote Robotic Hydro-erosion to produce rougher surfaces than pneumatic chipping hammers and hence improve mechanical interlocking, which in turn promotes bond strength.

- Further work is needed for the proposed method to become fully portable for in-situ evaluation of concrete substrates. Additional measurements (including the evaluation of 3D roughness parameters) are required for performing comparisons against traditional methods (sand patch method) and highly advanced 3D laser scanners. Finally, it should be noted that more advanced digital cameras with higher specifications than the one used in this study, can provide higher resolution images and hence improve the accuracy of the 3D reconstructed surface.

References

[1]   A.M. Neville, Properties of Concrete, fifth ed., Harlow, Essex, Pearson Education Limited, 2011.

[2]   S. Mindess, J.F. Young and D. Darwin, Concrete, second ed., Upper Saddle River, Prentice Hall, 2003.

[3]   N.J. Dellate Jr, D.W. Fowler, B.F. McCullough and S.F. Grater, Investigating performance of bonded concrete overlays, J. Perform. Constr. Facil. 12 (1998) 62-70. http://dx.doi.org/10.1061/(ASCE)0887-3828(1998)12:2(62).

[4]   BS EN 1504-10, Products and Systems for the Protection and Repair of Concrete Structures-Definitions-Requirements-Quality Control and Evaluation of Conformity-Part 10: Site Application of Products and Systems and Quality Control of the Works. British Standards Institution, London (UK), 2003.

[5]   BS EN 1766, Products and Systems for the Protection and Repair of Concrete Structures-Test Methods-Reference Concretes for Testing. British Standards Institution, London (UK), 2000.

[6]   BS EN ISO 3274, Geometric Product Specifications (GPS)-Surface Texture: Profile Method-Nominal Characteristics of Contact (Stylus) Instruments. British Standards Institution, London (UK), 1998.

[7]   BS EN ISO 4288, Geometric Product Specification (GPS)-Surface Texture-Profile Method: Rules and Procedures for the Assessment of Surface Texture. British Standards Institution, London (UK), 1998.

[8]   F.B. Holt and G.R. Musgrove, Surface Texture Classification: A Guide to Pavement Skid Resistance. Special Publication, ASTM International, West Conshohocken (Pennsylvania State, USA), 1982 31-44.

[9] ICRI Technical guideline No. 03732, Selecting and Specifying Concrete Surface Preparation for Sealers, Coating and Polymer Overlays. International Concrete Repair Institute, Rosemont, Illinois (USA), 1997.

[10] ASTM D 7682, Standard Test Method for Replication and Measurement of Concrete Surface Profiles Using Replica Putty, ASTM International, West Conshohocken, (Pennsylvania State, USA), 2012.

[11] J. Silfwerbrand, Bonding between old and new concrete in structures loaded by static and time-dependent load, In: Proceedings of the International Conference on Adhesion Between Polymers and Concrete. France, 1986.

[12] A.I. Abu-Tair, D. Lavery, A. Nadjay, S.R. Rigden and T.M.A. Ahmed, A new method for evaluating the surface roughness of concrete cut for repair or strengthening, Constr. Build. Mater. 14, 2000, 171-176. http://dx.doi.org/10.1016/s0950-0618(00)00016-7.

[13] N.H. Maertz, A. Nanni, J.J. Mayers and G. Galecki, Laser profilometry for concrete substrate characterization prior to FRP laminate application, Concr Repair Bull 1, 2001, 4-8.

[14] M.F.M. Ahmed and C.T. Haas, The potential of low cost close range photogrammetry towards unified automatic pavement distress surveying, In: Proceedings of the 89th annual meeting of the transportation research board, Washington, DC, January 2010.

[15] P.M.D. Santos and E.N.B.S. Julio, A state-of-the-art review on roughness quantification methods for concrete surfaces, Constr. Build. Mater. 38, 2013, 912-923. http://dx.doi.org/10.1016/j.conbuildmat.2012.09.045.

[16] J. Hola, L. Sadowski, J. Reiner and M. Stankiewicz, Concrete surface roughness testing using nondestructive three-dimensional optical method, In: NDT for

Safety/Defektoskopie, Sec u Chrudimi, Czech Republic, 30 October-1 November 2012, 101-106.

[17]   G. Bitelli, A. Simone, F. Giraldi and C. Lantieri, Laser scanning on road pavements: A new approach for characterising surface texture, Sensors 12, 2012, 9110-9128. http://dx.doi.org/10.3390/s120709110.

[18]   S. Warner, I. Neumann, K.C. Thienel and O. Heunecke, A fractal-based approach for the determination of concrete surfaces using laser scanning techniques: a comparison of two different measuring systems, Mater. Struct. 46(1-2), 2013, 245-254. http://dx.doi.org/10.1617/s11527-012-9898-y.

[19]   L. Sadowski, Application of three-dimensional optical laser triangulation method for concrete surface morphology measurement, Indian J. Eng. Mater. Sci. 21, 2014, 692-700.

[20]   J. Hola, L. Sadowski, J. Reiner and S. Stach, Usefulness of 3D surface roughness parameters for nondestructive evaluation of pull-off adhesion of concrete layers, Constr. Build. Mater. 84, 2015, 111-120. http://dx.doi.org/10.1016/j.conbuildmat.2015.03.014.

[21]   BS EN 197-1, Cement-Part 1: Composition, Specifications and Conformity Criteria for Common Cements, British Standards Institution, London (UK), 2000.

[22]   Design of normal concrete mixes, Garston: Building Research Establishment, second ed., 1998.

[23]   D. Chamberlain, A robotics approach to preparing surfaces for repair, Concr. 37, 2003, 22-23.

[24]   D. Chamberlain, E. Gambao, S. McCormac, M.A. Garcia, T. McCulloch, C.A. Alves Seibert et al., HEROIC: A concept robotic system for hydro-erosion in concrete repair

preparation. In: Proceedings of the 16th International Symposium on Automation and Robotics in Construction. Spain, 1999.

[25] E.S. Gadelmawla, M.M. Koura, T.M.A. Maksoud, I.M. Elewa and H.H. Soliman, Roughness parameters, J. Mat. Process. Technol. 123, 2002, 133-145. http://dx.doi.org/10.1016/s0924-0136(02)00060-2.

[26] B. Griffiths, Manufacturing Surface Technology, first ed., Penton Press, London, 2001.

[27] A.K. Bewoor and V.A. Kulkarni, Metrology and Measurement, first ed., McGraw-Hill, New Delhi, 2009.

[28] B.T. Meggitt, A new self-calibrating 3D interferometric fringe-based imaging system for profiling, positioning and control in space use. European Space Agency Final Report 15787/02/NL/PA, 2002.